

Nearest Particle Distance and the Statistical Distribution of Agglomerates from a Model of a Finite Set of Particles

J. Zidek^{1,2}, J. Kucera¹ and J. Jancar^{1,2}

Abstract: The structural analysis of a particulate composite with randomly distributed hard spheres is presented based on a model proposed earlier. The structural factors considered include the distribution of interparticle distances and the conditions for particle agglomeration. The interparticle distance was characterized by the nearest particle distance (NPD) and the distance derived from Delaunay triangulation (DT). The distances were calculated for every particle in the particle set and analyzed in the form of a cumulative distribution function (CDF). The CDF provides two parameters: the representation of particles which are in very close proximity to their neighbors and the most frequent distance between particles.

In the next step, the analysis of agglomerates was performed. The agglomerate was defined as a continuous unperturbed cluster of particles and interphase shells, which is divided from other clusters by a prescribed layer of matrix. The agglomerates were investigated from the point of view of their shape and size. Each set of agglomerates was analyzed by a histogram of agglomerate size and the average volume of agglomerates.

Finally, the agglomerate percolation was investigated. The percolation threshold was characterized by the size of agglomerate which can be considered the largest but still isolated, and the probability of percolation.

Keywords: particle distance, composite, percolation, agglomeration, Monte Carlo, effective volume.

List of symbols

Lower case

c_{red} Reduction coefficient for calculation of exact volume fraction of

¹ Brno University of Technology, Brno, Czech Republic

² Central European Institute of Technology, Brno, Czech Republic

	agglomerate (defined by the Eq. 4)
$c_{red,\infty}$	Reduction coefficient for infinite agglomerate
n_p	Number of particles in agglomerate = Size of agglomerate
l	Nearest particle distance (<i>synonym</i> <i>NPD</i>)
p	Percolation probability (Fraction of particles present in percolated network)
r_p	Radius of particle
t	Thickness of interphase layer; relative to particle radius in this paper
t	thickness of interphase/ r_{part}

Upper case

A, B, C	Partial radii of spherical subsets extracted from reference set (see V_{ref})
DT	Delaunay Triangulation
R	Radius of spherical reference set (see V_{ref})
F	Histogram of particle populations; $F(n_p, \phi_p, t)$ is population of particles in one data-set assigned to all agglomerates with size n_p .
NPD	Nearest particle distance; the value in this paper is related to average particle radius: $NPD = \text{Nearest particle distance}/r_{part}$
V_{agl}	Volume of agglomerate
$V_{agl,0}$	Volume of agglomerate obtained by simple summation of volume of all particles and interphase shells without considering intersection of interphases.
V_i	Volume of interphase shell
V_p	Volume of particle
V_{ref}	Volume of reference set, which contains all particles

Greek symbols

ϕ_p	Volume fraction of particles (without interphase) in the set
ϕ_{eff}	Effective volume fraction of particles with interphase in the set
ν	parameter steepness from <i>equation 5</i>

Phrases with numerical meaning

<i>Aspect ratio</i>	ratio of longest and shortest half axis of ellipsoid fitted to agglomerate
<i>Cumulative distribution function</i>	probability that a given property is less or equal than value on x-axis

<i>Effective volume (fraction)</i>	volume (fraction) of spheres in agglomerate including merged interphase layer
<i>Nearest particle distance</i>	distance between two surfaces of two nearest particles
<i>Percolation coefficient</i>	fraction of particles participating in infinite network
<i>Size of agglomerate</i>	number of particles in the agglomerate

1 Introduction

The distribution of particles in space is an important factor related to macroscopic properties of various materials. It can be investigated experimentally or by numerical models of hard spheres. The actual particle spatial distribution can be determined by various methods [Palik, (1975), Dietsch, (2006)]. The most current techniques, however, provide only 2D spatial distributions. By contrast, computer modeling enables the description of 3D distributions [Torquato (1995)].

The distance between particles and their distribution are important structural factors affecting macroscopic properties of particulate composites and strongly affect the relaxation behavior of glassy nanocomposites. For example, in the case of nanocomposites, the interparticle distances begin to be comparable to the radii of gyration of chains, and the chains may become constrained between nanoparticles at very low filler volume fractions. This effect is, in addition to the distribution of interparticle distances, strongly dependent on the nature of particle-chain interactions. Even in the case of weak interfacial interaction, the chain adsorption-desorption onto the particle surface is characterized by long relaxation times. Therefore, it seems useful to know the statistical and spatial distribution of the nearest particle distances, which can be used as input in models investigating the chain dynamics of polymer nanocomposites [Kalfus, Jancar, and Kucera (2008)].

The nearest particle distance between interpenetrable spheres spatially distributed according to an equilibrium ensemble was analyzed in a numerical simulation by Torquato and Lee (1990). They analyzed nearest particle distance in two limiting cases of interpenetrability: fully penetrable spheres and completely impenetrable (hard) spheres. Torquato (1995) compared the results with analytical equations. The derivation of an alternative numerical model generating a random distribution of hard monodisperse spheres of a given volume fraction in a reference sphere was presented by Zidek et al [Zidek, Kucera, and Jancar (2010)].

Agglomeration is a special case of the random spatial distribution of particles. The

agglomerates are formed by groups of particles close enough to act as an ensemble. In the space distribution of particles, the agglomeration can be described by the local fluctuation of particle density and introduced into the numerical model.

The effect of agglomeration on the macroscopic properties of particulate filled polymers was observed by Yanagioka and Frank (2008), and by Jancar, Kucera and Vesely (1988).

Yanagioka et al [Yanagioka and Frank (2008)] investigated two particle arrangements, namely the FCC lattice and the random spatial distribution. The elastic modulus of ordered nanocomposite was two times higher than the elastic modulus of random nanocomposite of the same concentration of filler. According to Bittmann, Hauptert, and Schlarb (2011), the toughness and elastic modulus of a nano-filled epoxy resin increased when the filler was dispersed by ultrasound during preparation. This effect can be ascribed to the breakage of nanoparticle agglomerates, which thus enhances the chain-particle interface area, resulting in an increase in the extent of chain stiffening.

However, agglomeration in microcomposites increases the stiffness of composites. This is interpreted as a result of the effective volume of agglomerates being higher than the sum of the volumes of all particles due to a portion of the soft polymer being trapped inside the agglomerate. This effect was observed experimentally and led to the modification of the Kerner-Nielsen theory, in which a simple geometrical constant is replaced by a function of agglomeration [Wu, Lin, Zheng, and Zhang. (2006)].

A model describing conditions for particle agglomeration was presented in literature as the penetrable concentric shell model by Lee and Torquato (1984, pp. 3258, pp. 6427). The model is composed of core particles which are completely impermeable and shells which are fully permeable. Two limiting cases were presented: totally impermeable spheres, and fully permeable spheres. Lee and Torquato (1984 pp. 3258) calculated the porosity by the Monte Carlo Method. They proposed an efficient method for calculating the total volume of particles with different grades of penetrability. Next, Lee and Torquato (1984 pp. 6427) derived a specific function detecting the isles of particles connected by intersecting interphase regions. The number of particles in one set was 512. The analysis of such a small particle set cannot distinguish individual numbers or representations of different agglomerates. In our model, we increased the number of particles to 100 000. Thus, statistical analysis could be performed also for agglomerate size and shape distributions. We could also calculate the thickness of the matrix interphase layer separating two agglomerates.

Particle agglomeration can be viewed as the first step towards particle percolation

observed at a certain volume fraction of conductive particles in conductive polymer composites. In general, the percolation is a state when randomly distributed elements in a given finite space form a continuous network [Grimmett (1999)]. It is supposed that each

particle has short connections to its neighbors. In the case of a small number of connections, only isolated clusters of particles are observed. When the number of short connections grows above a certain critical threshold, the interaction behaves as a long range one.

The percolation can be described mathematically by the percolation probability $\theta(p)$ of a certain state, p . It is the probability that the given element belongs to an infinite cluster. It is fundamental to the percolation theory that there exists some critical threshold value. It is assumed that below the critical value the percolation probability is zero, and that above the critical value the probability is a continuously growing function with a function value in the interval $(0,1)$:

$$\theta(p) \begin{cases} = 0 & p \leq p_c \\ = f(p) \in (0,1) & p > p_c \end{cases} \quad (1)$$

The percolation is not only a mathematical description of the structure. It has consequences for the macroscopic properties of materials. In many cases [see Garai, Chatterjee, and Nandi (2010); Bauhofer and Kovacs (2009); Kotsilkova (2007)], the transition between non-percolated and percolated states is accompanied by a steep change in properties (i.e. viscosity, elastic modulus, conductivity, etc.). This is why it is necessary to study parameters controlling percolation behavior in heterogeneous systems.

Many thermomechanical and physical properties of polymer nanocomposites suddenly change after reaching a critical filler concentration. In rheology, two critical concentrations, φ^* and φ^{**} , are proposed, called the first and the second percolation thresholds. These rheological parameters determine the qualitative structural transitions of nanocomposites with increasing filler content related to local and global percolation. The first percolation threshold (flocculation) expresses the critical concentration of local percolation and the formation of fractal flocks. The second rheological threshold (percolation) represents the formation of a continuous structural network of fractal flocks. The hard spheres model presented here also shows two transitions. The first percolation transition is observed when the network is created. However, only isolated clusters are present. The second percolation is observed when these clusters form a continuous network in at least one dimension.

The polydispersity of particle size and disorder of particles with respect to regular

space positions are structural factors which should be taken into consideration in the analysis. Polydispersity will be investigated in a follow up paper. Here, the particle spatial disorder is investigated in two limiting cases. The first is a set of particles which are maximally spatially disordered. The second is a set ordered in a cubic lattice.

The functions of the nearest particle distance and percolation ratio for a cubic network can be calculated analytically. Concerning the agglomerate, the situation is also relatively simple. The transition from isolated to percolated state is sharp; the particles will be either all isolated or all assigned to one agglomerate when the nearest particle distance becomes shorter than the critical percolation distance. The limit thickness, t , of the interphase for the isolated/percolated state is numerically equal to half of the nearest particle distance at the percolation threshold (*Tab. 1*).

Table 1: imensionless nearest particle distance, NPD, and thickness limit of interphase, t , relative to the particle radius for a cubic lattice as a function of the volume fraction of particles

ϕ_p %	NPD	t
1	5.48	2.74
2	3.94	1.97
5	2.38	1.19
10	1.47	0.74
20	0.76	0.38
30	0.41	0.21

The situation for randomly distributed particles is more complicated. The nearest particle distance and agglomerate analysis give, in this case, different information. The nearest particle distance gives information about the short-range particle distribution, whereas the agglomerate analysis gives information about longer range distribution.

The characteristics have to be calculated from a statistically significant set of particles and the result for the nearest particle distance can be described by a cumulative distribution function. Further, the frequency of agglomerates, aspect ratios of agglomerates, volumes of agglomerates and percolation transition can be calculated.

The percolation of a finite set of particles was investigated in a similar way by Rintoul and Torquato (1997). The percolation was investigated on a set of overlapping spheres. The spheres expanded from random points until reaching a certain volume fraction. The clusters were formed around their intersections. Two cases of percolation were defined: wrapping and spanning. In the wrapping case, the system has

to form the cluster from one side of the system to the other. In the case of spanning, the cluster must overlap with itself, when periodic boundary conditions are set.

Sanyal, Goldina, Zhub, and Kee (2010) presented the prediction of effective conductivity within porous composite electrodes. The conductivity was predicted by models of randomly packed spheres in a cubic box. They also defined percolation as a cluster spanning the box.

A common approach is the combination of the random packing of spheres with the Finite Element Method [Gurrum Zhao, and Edwards (2010)]. They modeled the Young modulus, Poisson's ratio and the coefficient of thermal expansion of heterogenous materials. Such simulations represent significant improvements on the results obtained for models considering spatially ordered particles.

2 Method

In this contribution, sets of 100 000 randomly generated spheres with a uniform size of particles and a prescribed volume fraction were generated. All the particles were packed in the space of a large reference sphere. The generated model data were:

- coordinates of particle centers and
- particle radii.

The generated model data were used as input data for the analytical phase, which is described in this paper.

Several structural factors were analyzed: nearest particle distance and agglomerate shape and size.

The random sets of particles were generated with volume fractions: 3×10^{-4} , 1.0, 2.0, 5.0, 7.5, 10.0, 12.5, 15.0, 12.5, 15.0, 17.5, 20.0, 22.5, 25.0, 27.5 and 30 % of volume respectively.

Each volume fraction was generated in five modifications: with interphase layer $t = 0.01 \times r_p, 0.05 \times r_p, 0.1 \times r_p, 0.2 \times r_p, 0.5 \times r_p$, where r_p is the radius of particles.

For each combination [volume fraction \times interphase layer] 10 independent particle sets were generated.

2.1 Generation of a spherical set

The set of particles was generated by in house software based on the Tovmasjan (1986) method. The first step was the generation of a given number of randomly distributed particle centers in a given reference sphere. The two following operations were then performed. First, an inflation of particles was undertaken. The

inflation of particles led to an increase in the particles' volume. This was possible at low volume fractions. When the volume fraction grew, the intersections of particles occurred. The second operation then consisted in the elimination of particle intersections by pushing out the particles. The procedure progressed from the center of the sphere to its boundary. In the case that intersecting particles were detected, the outer particle (of greater distance R to the mass center of the particle set) was pushed out by the inner particle. The macroscopic homogeneity was verified by radial distribution functions. The radial distribution function of the generated spherical set was inside theoretical boundaries.

The particle sets were investigated from the points of view of nearest particle distance and Delaunay triangulation (DT). The nearest particle distance is the distance to the nearest particle.

The Delaunay triangulation of particle centers was performed by a Qhull algorithm [Barber, Dobkin, and Huhdanpaa (1996)].

2.2 Concept of agglomerates

The basic model of an agglomerate is based on particles with an interphase layer. It was presented in the literature as the penetrable concentric shells (PCS) model (cherry-pit model) [Lee and Torquato 1988. pp. 3528].

The model presented in this paper extends the possibilities of the PCS model. It is composed of a large number of particles, with accelerated algorithm. An agglomerate is an unperturbed continuous object inside the model composed of particles and interphase shells. The number of agglomerates in the model was lower than the number of spheres. However, it was still large enough for the statistical analysis of agglomerates. Data about the size and shape of agglomerates and the nearest distance between agglomerates were taken from the statistical set of agglomerates.

The agglomerates were constructed using the following algorithm. The interpenetrable layer has a thickness t . When the interphase layers of two particles are intersecting or touching, they are agglomerated. Two agglomerated particles create a volume delimited by the volume of selected particles and the volume of their interphase layers, see *Fig. 1*. In the case of the intersection of the interphase of a third particle with one or two agglomerated particles, the third particle is included into the agglomerate. The fourth, fifth, \dots , n^{th} particle are added when their interphase intersects the interphase of one particle just present in the agglomerate. *Fig. 1d* shows the union of volumes.

Such a concept of an agglomerate has several limitations. One of the major limitations is shown in *Fig. 1*. Some volume segments (gray A in *Fig 1 d.*) are, in reality, in the agglomerate, but in the model the volume is outside the agglomerate.

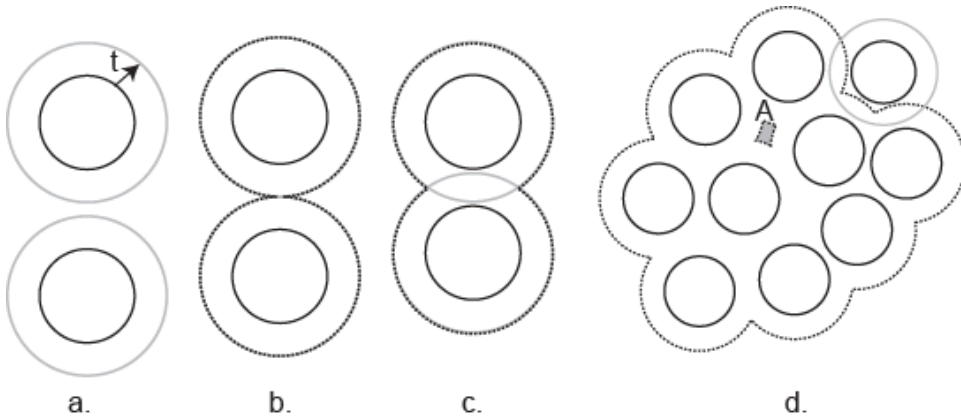


Figure 1: concept of agglomerate; Particle -black solid line and interphase (gray line); Basic condition a - separated particles (not agglomerated); b,c possible agglomerates - (b-contact ; c-intersection); d - addition of next particle to existing agglomerate. A - volume existing in a real agglomerate but not detected by the model.

In our study, the particles sorted to the agglomerate had a flag – “classified to certain of agglomerate”. (If it happened that a particle did not have any close neighbor particle, the particle was considered a “one-particle” agglomerate.) Then, the first non-classified particle nearest to the center of gravity was found again. The procedure was repeated until non-classified particles were present in the set. The primary results of this process were tables of particles (centers and radii) in each agglomerate.

2.3 Calculation of volume fraction by the Monte Carlo method

The agglomerate has an irregular shape. It is composed of particles and intersecting interphases of particles of the agglomerate. The volume of such a system cannot be meaningfully calculated analytically. The volume of agglomerates was calculated by the Monte Carlo (MC) method (Eq. 2).

$$D = \int_D f(x) dV = D' \frac{N}{N'} \quad (2)$$

where $[\forall x \in V, f(x) = 1; \quad \forall x \notin V, f(x) = 0]$.

The calculation of the volume is an application of the Monte Carlo [Dimov (2008)] integration method. In order to integrate a function over a complicated domain D ,

Monte Carlo integration picks random points over some simple domain D' which is a superset of D . The method estimates the volume of D as the volume of D' multiplied by the fraction of points falling within D' .

Picking N randomly distributed points $\mathbf{x} = (x_1, x_2, \dots, x_n)$ in a multidimensional volume to determine the integral of a function in this volume gives a result.

In short, the calculation of volume by the MC method is provided by the generation of random points in a box. The investigated object is inside the box. The number of points in the investigated object, the number of all points, and the volume of the box are used to calculate the investigated volume. The law of large numbers ensures that the Monte Carlo estimate converges to the true value of the integral. The error estimate of a Monte Carlo integration is of the order of $1/\sqrt{N}$.

The calculation of the model volume fraction of a cherry model is described in papers by Lee and Torquato (1988).

Our procedure is adapted to models with a large number of particles. The objects of particles were sorted by treesort algorithm to one segment of random access memory (RAM). The sorting criterion was distance from mass center. Then, the random points were sorted to a linked list data structure. The criterion was also the distance from mass center. Each random point delimited certain sub-segment of memory, where all possible intersecting particles are. The sub-segment was bounded by two pointers to the segment of memory. One pointed to a lower boundary stop and the second one to an upper boundary stop of the block. Then, the presence of a point inside the particle was tested only for selected particles in the sub-segment. It was significantly smaller than the all-particle segment.

The investigation of the next random point was performed by data structures created by its predecessor. The following random point was found in the linked list as the next one to the actual random point. Then, the sub-segment of memory, in which were written the corresponding particles, was shifted. (All particles were placed in the same segment of memory. Only the pointers which marked the lower and upper boundary of the sub-segment were shifted. Next, the presence of new random point in any particle was tested.

2.4 Aspect ratio of agglomerates

The aspect ratio is a property which characterizes divergence from a spherical shape. It was calculated by MATLAB script. It was calculated by the ellipsoid inscribed into the agglomerate, where the volume of the ellipsoid was equivalent to the volume of particles with interphase layers. The ellipsoid prescribed the same volume as the agglomerate. The optimum set of ellipsoid axes was found by maximizing the intersections of two volumes: 1. of the agglomerate and 2. of the fitted

ellipsoid. The results of optimization were three semi-axes as parameters. Then, the ratio of the longest and the shortest semi-axis was considered as the aspect ratio. The local maxima of volume were found searched by the function f_{min}^{search} utilizing MATLAB. This function uses a simplex search method for the numerical searching of local extremes.

3 Results and Discussion

Ten particle sets were generated for each particle volume fraction. The sets were analyzed from the viewpoints of particle distances and agglomeration. The volume fraction of agglomerates in the randomly spatially distributed particles generated in the simulation sphere is given by Eq. (2).

3.1 Nearest particle distance

The nearest particle distance was calculated as the distance between the spherical surfaces of the nearest particles. The result of the calculation was processed as a cumulative distribution function for each volume fraction (*Fig. 2*). One cumulative distribution function was calculated for each volume fraction.

The curves from *Fig. 2* can be described by two parameters: the inflection point and the limiting CDF obtained for $l/r_p \rightarrow 0$. Both parameters have real physical meaning. The inflection point means the distance between particle surfaces (related to particle radius) which is the most frequently represented in the model. The limiting value means the portion of nearest particles which are in close proximity to their neighbors.

Simultaneously, the distances from Delaunay triangulation (DT) were calculated. The curves from DT have the same shape as the cumulative distribution function of NPD. The functions from DT are shifted from the curves for NPD. The inflection point is shifted to longer distances and the lim CDF $l/r_p \rightarrow 0$ is lower for DT. The results are compared in *Table 2*.

There is a difference between distances calculated from DT and NPD. The distances from DT are the set of distances between a certain central particle and particles in its proximity. The NPD is formally a selection distance between a given particle and its nearest neighbor. This means that the most frequent distance (inflection point) must be lower for NPD. Also, the representation of spheres in close contact is lower. The absolute number of very narrow distances is similar in both NPD and DT. However, the complementary number of greater than nearest distances is much higher in DT than in NPD. This is why the relative representation of close distances in DT must be lower than in NPD.

For example, at a 2% volume fraction of particles, the representation of close parti-

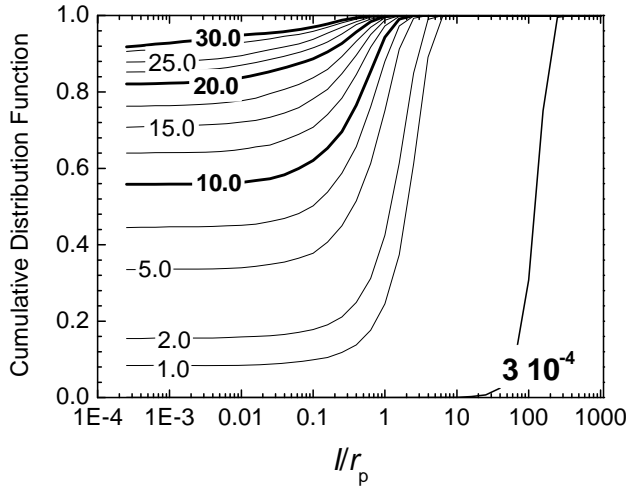


Figure 2: Cumulative distribution function of nearest particle distances; l/r_p - the nearest particle relative to the particle radius; numbers on lines represent the volume percentage of particles.

cles in NPD was approximately 14 times higher than in DT. Yet, at 30% of volume, the representation of close particles from NPD was only 5.5 times higher than in DT. This is because at high volume fractions, one particle can be surrounded by two or more particles in close proximity. In the case of the closest spatial arrangement of monodisperse spherical particles (74.05 % by volume), both the representations of very close particles (from NPD and DT) should be equal to 1.

The results were compared with the boundaries presented by Torquato (1995). He presented a theorem valid for any ergodic and isotropic packing of identical D-dimensional hard spheres ($D=3$):

$$\bar{l}/r_p \leq \frac{2}{D 2^D \phi}, \quad (3)$$

where l is the mean interparticle distance. If the particles do not satisfy this condition, they cannot be ergodic and isotropic. All the particle sets in our simulations satisfied this condition. The mean distances were calculated directly from the sets of all distances. However, they are not presented in this paper. The mean distance can be calculated approximately as an average of the number of “zero distances”, the number of non-zero distances, and the most frequent non-zero distance:

$$\bar{l}/r_p \approx [1 - CDF_{(l \rightarrow 0)}] \text{ Inflection } p. \quad (4)$$

Table 2: Parameters of cumulative distribution functions CDF (from Fig. 2); Comparison of Nearest Particle Distance and Delaunay Triangulation

φ_p	Nearest Particle Dist.		Delaunay Triang.	
	Inflection point	CDF ($1/r_p \rightarrow 0$)	Inflection point	CDF ($1/r_p \rightarrow 0$)
$3 \cdot 10^{-4}$	129.978	0.00	295.400	0.00
0.010	2.489	0.08	7.668	0.01
0.020	1.758	0.14	6.252	0.01
0.050	0.891	0.33	4.169	0.03
0.075	0.834	0.45	3.436	0.04
0.100	0.656	0.56	2.897	0.06
0.125	0.531	0.65	2.582	0.08
0.150	0.460	0.72	2.291	0.09
0.175	0.398	0.77	2.133	0.11
0.200	0.331	0.83	1.871	0.12
0.225	0.316	0.85	1.714	0.14
0.250	0.297	0.89	1.567	0.15
0.275	0.252	0.92	1.466	0.16
0.300	0.214	0.95	1.358	0.17

It more or less corresponds to the mean distance, which was calculated directly from the set of distances.

Next, the mean values were compared to the analytical equation for hard spheres in equilibrium presented by Torquato (1995). Our mean NPD was significantly lower than the distance presented by Torquato. This means that we generated a model different from the hard spheres equilibrium model. However, the model also passed the criteria of ergodicity and isotropicity. We also found [Zidek, Kucera and Jancar (2010)] that the radial distribution functions of our models were inside the boundaries valid for the random distribution of spheres. Such models can also be considered as random, even if they are significantly different from random systems presented in the literature. Therefore, for one volume concentration of spheres, further different random models can be generated with the model we derived.

3.2 Histograms of agglomerates

A histogram of agglomerates gives information about the number of agglomerates in the model. The agglomerate was constructed by the method from *Section 2.1*. Agglomeration was investigated for sets of 100,000 particles of different volume fractions and with different thicknesses of interphase. Examples of such a his-

togram are shown in *Figs. 3 and 4*. *Fig. 3* shows the influence of volume fraction on the histograms with $t/r_p = 0.01$. *Fig. 4* shows the histograms for the same volume fractions as in *Fig. 3* with an interphase of $t/r_p = 0.1$.

It is clear that the higher the volume fraction of particles and the thickness of interphase, the larger the agglomerates that will be observed. The question is whether the same effect can be achieved simply by increasing the effective volume. It is not important whether it is reached by increasing the interphase thickness or increasing the volume fraction of particles.

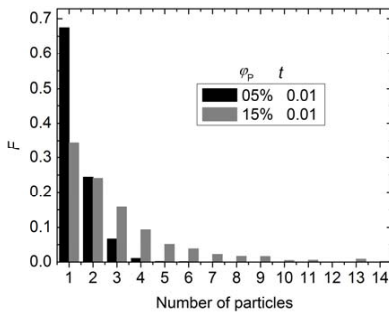


Figure 3: Histogram of agglomerates sizes (number of particles in agglomerates) for two different volume fractions and constant thickness of interphase 0.01 r

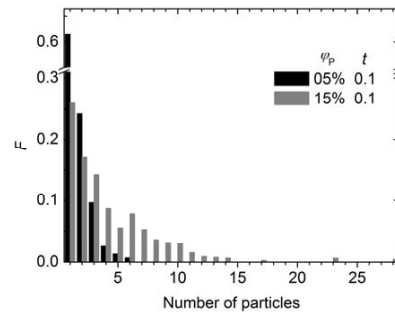


Figure 4: Histogram of agglomerates sizes for two different volume fractions (the same fractions as in *Fig. 3*) and constant thickness of interphase 0.1 r

It must be highlighted that the histograms are meaningful only for the non-percolated state. The percolation will be analyzed in *Section 3.5*. In the percolated state, the histogram will be replaced by a single parameter: the coefficient of percolation (see Appendix).

3.3 Calculation of volume fraction by the Monte Carlo method

As mentioned above, the thickness of interphase and volume fraction of particles can be replaced by a single parameter – effective volume. It is the volume created by uniting the volume of the particles and the volume of the interphase layers. The volume of agglomerates is irregular; therefore, in our study, it was calculated by the method Monte Carlo. 10^{10} random points were generated in the reference sphere. The volume was calculated from the number of random points which were detected inside the particles or interphases. Then it was possible to estimate a coefficient

describing the intersection of interphase layers. The coefficient can be evaluated in following way. First, we calculate the unintersected volume of agglomerates simply as the sum of volumes of particles and spherical interphase shells (as they are not intersected):

$$V_{agl,0} = \sum (V_p + V_i) = 4/3\pi (r_p + t)^3. \quad (5)$$

The volume reducing coefficient is then defined as the ratio of the real volume of a given agglomerate and the unintersected volume.

$$c_{red} = V_{agl}/V_{agl,0}. \quad (6)$$

The reduction coefficients for different thicknesses of interphase layers are shown in *Fig. 5*. The graph also shows a relatively high standard deviation for agglomerate volume. It is caused by different degrees of interpenetration of interphase layers.

As shown in the construction of agglomerates in *Fig. 1b*, the agglomerate can be relatively sparse, because several particles can form the agglomerate even if their interphases only touch. This has the consequence that many of the interparticle spaces which are, in reality, inside the agglomerate are not counted in the agglomerate model. This is why the complex interphase was defined, i.e. the interphase layers overlap significantly and internal free volumes in agglomerates are reduced. The function of the reduction coefficient on agglomerate size in this case is shown in *Fig. 6*. The interphase used for the calculation of volume has twice the thickness of the interphase layer used for construction.

This shows that every function of the reduction coefficient on the size of an agglomerate can be approximated by an exponential function:

$$c_{red}(n_p, t) = c_{red,\infty}(t) + [1 - c_{red,\infty}(t)] \cdot \exp\left\{\frac{1 - n_p}{v}\right\} \quad (7)$$

where $c_{red,\infty}$ is the reduction coefficient for an infinite agglomerate and v is the parameter of steepness of the function.

The coefficient of steepness is independent of thickness of interphase and is similar for every data series with a given thickness and interphase type $v = 2.76 \pm 0.21$.

Differences in individual data sets are only in the value of the single parameter: $c_{red,\infty}$. This parameter represents the reduction coefficient which must be applied to an infinite agglomerate. It will be used for the calculation of the effective volume of percolated agglomerates. The function of infinite reduction coefficient depending on thickness of interphase is shown in *Fig. 7*.

The combination of two functions, the histogram and the reduction coefficient, enables us to calculate the effective volume of an arbitrary particle system which

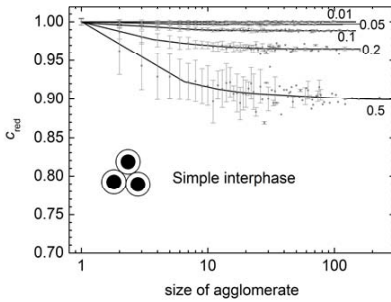


Figure 5: Reduction coefficient (c_{red}) for calculation of volume of agglomerate from Eq. 6; Dependence on size of agglomerates for different thicknesses of interphase layers (t- number at lines). The interphases are considered only as in simple contact

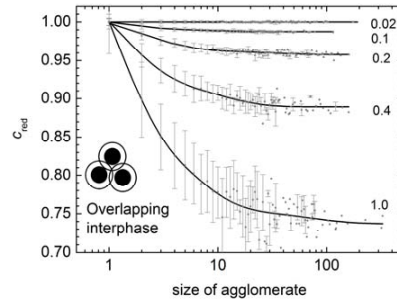


Figure 6: Reduction coefficient (c_{red}) for calculation of volume of agglomerate from Eq. 6; Dependence on size of agglomerates for different thicknesses of interphase layers (t- number at lines). The case when interphases are significantly overlapping

is not percolated. Examples of histograms are shown in *Figs. 3* and *4*, and the result is a discrete function of the frequency of particles depending on the number of particles in an agglomerate. The frequency has the following two parameters: the volume fraction of particles and the thickness of interphase: $F(n_p, \varphi_p, t)$.

The reduction coefficient from *Figs. 5* and *6* depends on the number of particles in the agglomerate and the thickness of interphase $c_{red}(n_p, t)$.

The parameters φ_p and t are, together, two parts of such an effective volume of filled polymer. The aim is to find whether it is possible to reduce the parameter set of histograms only to the effective volume fraction of particles: $F(n_p, \varphi_p, t) = F(n_p, \varphi_{eff})$.

The effective volume of all particles in a certain reference volume is calculated from the volume of particles, their frequency, and thickness of interphase:

$$\varphi_{eff}(\varphi_p, t) = \frac{\sum_{np=1}^{np, \max} [c_{red}(n_p, t) \cdot F(n_p, \varphi_p, t) \cdot V_p]}{V_{ref}} \quad (8)$$

After processing, this equation becomes:

$$\varphi_{eff}(\varphi_p, t) = (1+t)^3 \varphi_p \sum_{np=1}^{np, \max} [c_{red}(n_p, t) \cdot F(n_p, \varphi_p, t)] \quad (9)$$

The calculation of effective volume can help with the question of whether it is possible to reduce the parameter set from a two parameter set $[\varphi_p, t]$ to a single parameter - φ_{eff} . From all the calculated data sets, the data sets which have different volume fractions of particles (φ_p), but a similar effective volume fraction (φ_{eff}) was selected. Their histograms are compared in *Fig. 8* and they are similar.

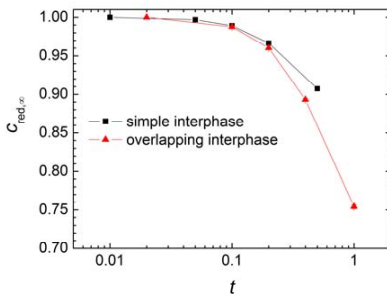


Figure 7: Reduction coefficient for calculation of volume of agglomerate $C_{red,\infty}$, whose size is approaching infinity - function of interphase thickness t . Values were calculated (by Eq. 7) from exponential extrapolation of data from *Figs. 5* and *6*.

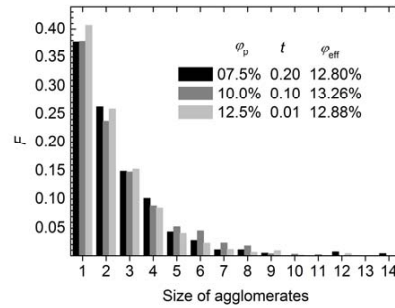


Figure 8: Histograms of size of agglomerates for three different particle sets with similar effective volumes of agglomerates.

3.4 Aspect ratio of agglomerates

The aspect ratio is a geometrical factor of an agglomerate. It gives information about the agglomerate shape. The aspect ratio can theoretically be in the range from 1 (an ideal sphere) to ∞ for a long infinite fiber. In several systems, particle agglomerates are formed with a shape of chain of large aspect ratio. In our case, agglomerates of grape shape were observed. It was presumed that the shape was slightly elongated and that the shape could be approximated to an ellipsoid as shown in *Fig. 9*.

The aspect ratio was calculated as the ratio of the longest axis to the shortest axis and was investigated as a function of agglomerate size (see *Fig. 10*). It was found that the aspect ratio does not depend on the volume fraction and interphase thickness (*Fig. 11*).

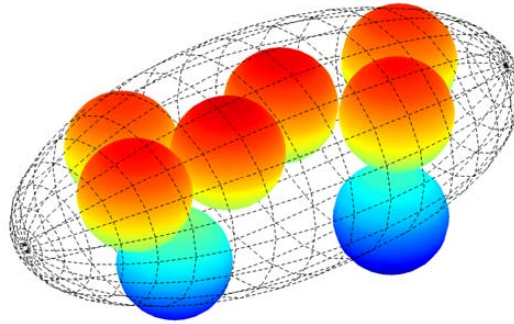


Figure 9: Substitution of an agglomerate by an ellipsoid; the semi-axis lengths were derived from the combined volume of the ellipsoid and the particles; the surface color of particles (or degree of gray) was used only to increase the 3D impression.

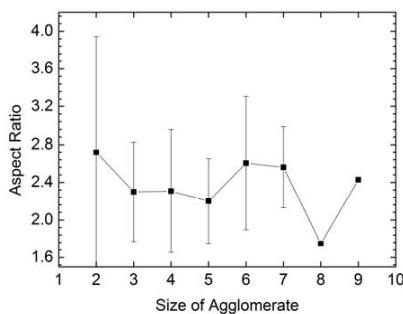


Figure 10: Aspect ratio as a function of agglomerate size for one generated set of particles with a volume fraction of 0.05 and interphase thickness of 0.1.

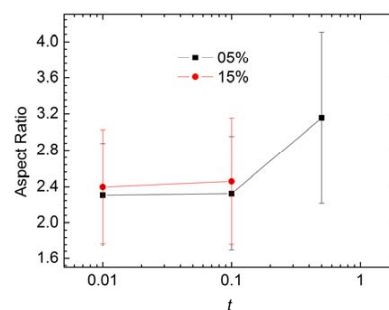


Figure 11: Mean aspect ratio for generations with different volume fractions of particles and interphase layers t

The result of this analysis is that all the agglomerates are approximately slightly elongated ellipsoids and the shape is independent of other structural properties.

3.5 Percolation

During the analysis, it was found that the boundary of a particle set distorts the analysis of agglomerates. This is the case with agglomerates whose size is unascertainable. The accuracy can be increased when the boundary particles constitute a

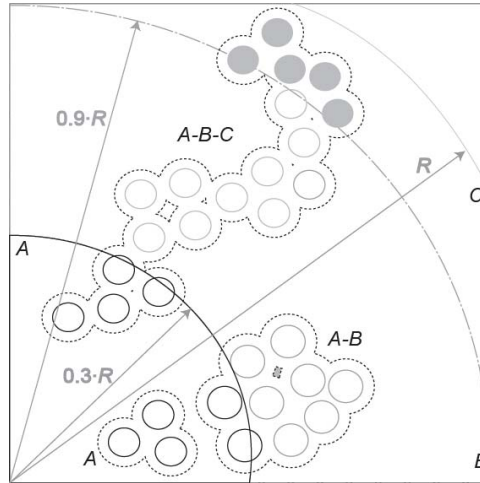


Figure 12: Definition of percolated state; Particle set divided into 3 layers A, B and C; 3 possible types of agglomerates detected by analysis: A - isolated agglomerate; A-B - partly isolated agglomerate; A-B-C - percolated agglomerate not analyzed by the histogram; particles in set; R- boundary of generated particle set.

very small fraction of all particles. This is in the case of a large number of particles in combination with small agglomerates. However, in our generated sets large agglomerates were also present. A function which determined whether the agglomerate was large and still isolated, or infinite and just percolated was needed. As stated in *Section 1*, the percolation is the transition when the isolated agglomerates intergrow into one percolated network. The limitation of our numerical model was that the model (reference sphere) is always finite. Due to the generation procedure, it was not possible to build a periodic box. All the particles were found in a large reference sphere of radius R . As the particle distribution was homogenous, some subset could be extracted from the reference set. The particles outside the subset boundary have to have the same spatial distribution as the particles inside the selected set. A small inner sphere of radius $0.3R$ was selected from the all-particle set with a reference radius R (*Fig. 12* sphere *A*). The agglomeration was checked in each new case from the particles inside subset *A*. The particles outside subset *A* could join the agglomerate started in subset *A*, if they satisfied the condition for agglomeration (*Fig. 1*). The evaluation of the analysis was simple until agglomerates were formed exclusively from particles inside *A*. When some particles from outside *A* participated, a next step in the analysis was performed.

The outside space was divided into the following two subsets *B* and *C*. Subset *B*

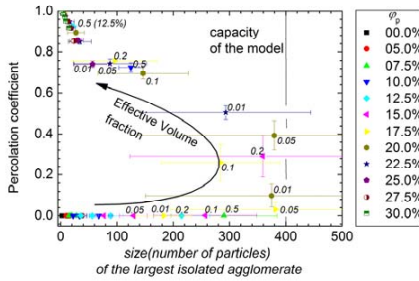


Figure 13: Percolation coefficient of agglomerates in percolated state; dependence on maximum isolated agglomerate in the set; different volume fractions of naked particles (ϕ_p) are highlighted in the graph.

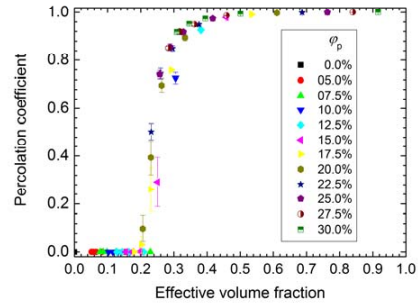


Figure 14: Percolation coefficient as a function of effective volume fraction of agglomerates; different volume representations of naked particles (ϕ_p) are highlighted in the graph.

was defined from radius $0.3R$ to radius $0.9R$ and subset C was from $0.9R$ until the absolute boundary of the set of all particles ($1.0R$).

As stated above, the agglomerates analysis always started in subset A . The cross-boundary agglomerates either stopped in B or grew into C . If they stopped in B , they were considered isolated. The agglomerate was recorded in the histogram in a special way. The size of agglomerate (x -axis) was the number of particles in A and B together. However, the count of particles (y -axis) was increased only by the number of particles in A . It was the same situation as if the binary decision about the agglomerate (present/absent in the range A) was replaced by the decision “partly present” in the range of A .

When the agglomerates grew into layer C , the state was considered percolated. The representation of such an object was again counted using the particles only present in A , as in the previous case. However, the number of particles in the agglomerate was set to infinity. In addition, if several such (A - B - C) objects in one set were detected, they were taken as one object with a representation equal to the sum of all partial representations. The representation of percolated particles related to all particles in subset A was used for the calculation of the percolation coefficient p . The percolation coefficient p is, in fact, the fraction of particles from all particles which participate in the infinite percolated network of particles.

The percolation was investigated for different volume concentrations of particles in

the range from 0% to 30% of naked particles. Each concentration was investigated with an interphase layer thickness equal to 0.01, 0.05, 0.1, 0.2, and 0.5 respectively. Each combination of volume fraction and thickness of interphase was analyzed by 10 independently generated particle sets of 100,000 particles. The mean values and standard deviations of size of the largest agglomerate and the percolation coefficient were calculated.

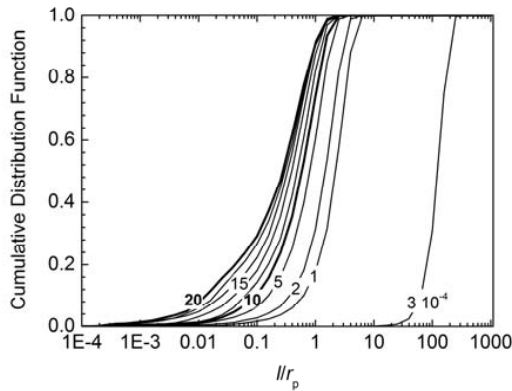


Figure 15: Cumulative distribution functions of nearest agglomerate distances; compare to Fig. 2.

Two properties related to the percolation were analyzed: the size of the largest detected isolated agglomerate in the subset A and B (*Fig. 13* - x axis) and the percolation coefficient (*Fig. 13* - y axis). Of course, both the properties are related to the given model of spheres and the settings of boundaries of subsets A, B and C from *Fig. 12*. A change of model settings will lead to different numerical values, but their functions should be similar.

The limiting size of the largest isolated agglomerate (≈ 400 particles) is a property which detects the starting point of percolation transition. Larger agglomerates are indistinguishable from percolated agglomerates. It is a transition in which an isolated agglomerate grows out of the investigated part (A and B) of the model. This state was considered to be near the first percolation threshold. Outside the investigated region (A and B) we can imagine some copies of our investigated systems. If the agglomerates of copied systems grow out of the boundary, they have to meet together with agglomerates of the investigated system and form a continuous network of particles. However, there is still a significant portion of isolated agglomerates.

The growing out and collisions of agglomerates are observed until a percolation ratio of 0.5 is achieved.

Above this value ($p > 0.5$), the capacity of a model to create large isolated clusters is exhausted. The character of the percolation changes. Let us consider particle by particle addition to a system in which some sparse percolated network of particles exists. The coalescence of large agglomerates starts in the investigated system. This is why the large agglomerates disappear. In the projection to the infinite system (the investigated system and its copies around), this corresponds to the creation of new connections in the existing network. The density of the particle network will increase until the second transition. At the second percolation threshold, the isolated clusters disappear completely and all particles start to be in one percolated network.

Numbers beside symbols are thicknesses of interphase layers (relative to particle radius- t/r_p). $N_{p,max} \approx 400$ is the capacity of the model to form isolated agglomerates; its value depends on the number of particles in the generated set and the settings of the model boundaries A and B from *Fig. 12*.

The path of the arrow in *Fig. 13* represents a warped axis of the effective volume fraction. It also has a deformed shape and scale. The projection of data onto the effective volume fraction axis is shown in *Fig. 14*. The effective volume fraction is derived as in *Eq. 9*. In contrast to the equation, in the percolated state, a single infinite agglomerate is present:

$$\varphi_{eff}(\varphi_p, t) = (1 + t)^3 \varphi_p c_{red,\infty}(t) \quad (10)$$

The reduction coefficients $c_{red,\infty}$ for infinite agglomerates can be found in *Fig. 7*.

The percolation is zero at low effective concentrations, then increases steeply between effective fractions of 0.2 and 0.3 until full percolation is achieved. Above a concentration of 50%, the percolation of all-particles is observed.

3.6 Combination of nearest particle distance and agglomerates

It is evident that in the case when the effect of the particle agglomeration in the material is observed, it is necessary to revise the expression of the function of particle distance (*Section 3.1, Fig. 2*). If the particles are too close, the particles whose critical distance is lower than a critical distance form an agglomerate. Such an agglomerate behaves in the system like an independent structural object. This is why it is better to consider the minimum “free” distance in a composite as the smallest distance between particles which are not in the same agglomerate. That is, for each particle, a nearest particle was calculated, which was assigned to a different agglomerate and the distribution of such distances was recalculated. An example

is shown in *Fig. 15*, where the distribution was calculated for volume fractions of particles up to 20% and a very thin interphase layer ($10^{-4}r_p$). This was the thickness of layer which was thick enough to filter out small distances in small closely grouped agglomerates. However, it was thin enough so that percolation under 20% of volume was not achieved. In *Fig. 2*, the lowest fraction of nearest neighbor distances ($l/r_p = 10^{-4}$) is highly populated. It can be deduced that the lowest fraction of nearest neighbor distances has a lower population and that a significant population is observed at higher distances. However, in this case, also, the distances between agglomerates are very small. Above a concentration of 17.5%, the cumulative distribution functions of agglomerates are deformed. This is because there are a significant number of inner particles which are closely surrounded only by particles from the same agglomerate. The nearest particles from neighboring agglomerates are then relatively far away.

4 Conclusions

The paper describes the analysis of a numerical model of 100,000 spheres, which occupy a volume cell of defined volume fraction. The volume fraction of spheres was from 0 to 30%. Non-intersecting hard monodisperse spheres were randomly distributed in space. An interphase layer of defined thickness was projected around each particle. The agglomerate was composed of locally grouped particles whose interphase layers were merged. The shape and size of agglomerates were investigated.

Concerning the shape, the aspect ratio was found to be 2 with a large degree of variance. This value was observed independently of agglomerate size. This means that the agglomerates usually have the shape of slightly elongated ellipsoids, but their shapes can vary from a sphere to a jet-shape. They did not form any chainlet or fiber structures.

The distribution of agglomerate size depended on the effective volume (the volume of all particles and the merged interphase layer). The histograms of agglomerate size were similar for sets with similar effective volumes of agglomerates, even if the volume fractions of core particles were different.

If the volume fraction of particles increased, percolation was observed. This was the state in which isolated agglomerates grew out to the continuous network of particles. The histograms were replaced by a single constant: the percolation coefficient. It is the fraction of spheres (from all spheres) participating in the independent continuous network. In the first stage of percolation, the network of particles was just formed, but there were still isolated agglomerates. In the next stage, the remaining isolated agglomerates merged with the existing continuous network. They

joined the network. The final stage was the stage in which all particles form a continuous network. The fraction of isolated/percolated particles depends only on the effective volume fraction of agglomerates.

Concerning the nearest particle distance, the particles are relatively close to their nearest neighbors. This is observed even with low volume fractions of particles. If the agglomeration is introduced, the gaps between particles from two neighboring agglomerates are much larger. The analysis is meaningful for volume fractions lower than 20%. Above this value, the applied simple analysis is distorted.

The paper also presents a set of parametrical equations valid for such types of models (models in which the particles have a tendency to form clusters). The parametrical equations enable the numerical expression of mean distance between particles (Eq.4), the volume of agglomerates (Eq.7), and the effective volume fraction of a percolated network of particles (Eq.10).

All the conclusions were tested for systems with monodisperse spheres. The effect of polydispersity will be investigated in further papers.

Acknowledgement: This research was supported by the Grant Agency of The Czech Republic under the project GA106081409 and by the Ministry of Education of the Czech Republic under research project MSM 0021630501

References

- Barber, C.B.; Dobkin, D.P.; Huhdanpaa, H.T. (1996):** The Quickhull algorithm for convex hulls, *ACM Trans. on Mathematical Software*, vol. 22, pp. 469-483.
- Bauhofer, W.; Kovacs, J. Z. (2009):** A review and analysis of electrical percolation in carbon nanotube polymer composites, *Composites Science and Technology*, vol. 69, no. 10, pp. 1486-1498
- Bittmann, B.; Hauptert, F., Schlarb, A.K (2011):** Preparation of TiO₂/epoxy nanocomposites by ultrasonic dispersion and their structure property relationship, *Ultrasonics Sonochemistry*, vol. 18, no. 1, pp. 120-126.
- Dietsch, H. (2006):** *Nanoparticle Hybrid Systems Synthesis of a Tailored Composite Model*. Dissertation, University Freiburg (Schweiz).
- Dimov I.T. (2008),** *Monte Carlo methods for applied scientists*. World Scientific Publishing, Danvers USA.
- Garai, A.; Chatterjee, S.; Nandi, A.K. (2010):** Viscoelastic and conductivity properties of thermoreversible polyaniline-DNNSA gel in m-cresol, *Synthetic Metals*, vol. 160, no. 15-16, pp. 1733-1739.
- Grimmett, G. (1999):** *Percolation*; 2nd edition Springer Verlag, Berlin, Germany.

- Gurrum, S.P.; Zhao, J.H.; Edwards D.R.** (2010): Inclusion interaction and effective material properties in a particle-filled composite material system, *Journal of Materials Science*, DOI: 10.1007/s10853-010-4844-2.
- Jancar, J.; Kucera, J.; Vesely, P.** (1988): Some peculiarities in viscoelastic response of heavily filled polypropylene composites, *Journal of Materials Science Letters* vol. 7, no. 12, pp. 1377-1378.
- Kalfus, J.; Jancar J.; Kucera, J.** (2008): Effect of weakly interacting nanofiller on the morphology and viscoelastic response of polyolefins, *Polymer Engineering and Science*, vol. 48, no. 5, pp. 889-894.
- Kotsilkova, R.** (2007): *Thermoset Nanocomposites for Engineering Applications*. Smithers Rapra Technology.
- Lee S.B., Torquato S.** (1988): Porosity for the penetrable-co-centric shell models of two-phase disordered media: Computer simulation results, *J. Chem. Phys.*, vol. 89, no. 5, 3258-3263.
- Lee S.B., Torquato S.** (1988): Pair connectedness and mean cluster size for continuum-percolation models: Computer simulation results, *J. Chem. Phys.*, vol. 89, no. 10, 6427-6433.
- Palik, E.S.** (1975): Characterization of Particulate Structures, *Powder Technology*, vol. 13, no. 1, pp. 9-14.
- Rintoul, M.D.; Torquato, S.** (1997): Precise determination of the critical threshold and exponents in a three-dimensional continuum percolation model; *J. Phys. A: Math. Gen.*, vol. 30, no. 16, pp. L585–L592.
- Sanyala, J.; Goldina, G.M.; Zhub, H.; Kee, R.J.** (2010): A particle-based model for predicting the effective conductivities of composite electrodes, *Journal of Power Sources*, vol. 195, no. 19, pp. 6671-6679.
- Torquato, S.** (1984): Bulk properties of two-phase disordered media. I. Cluster expansion for the effective dielectric constant of dispersions of penetrable spheres; *The Journal of Chemical Physics*, vol. 81, no 11, pp. 5079-5088.
- Torquato, S.** (1995): Mean Nearest-Neighbor Distance in Random Packing of Hard D-Dimensional Spheres, *Physical Review Letters*, vol. 74, no. 12, pp. 2156-2159.
- Tovmasjan, J. M.; Topolkarev, V.A.; Berlin, A. A.; Zhurablev, I. L.; Enikolopjan, H. C.** (1986): Structural organization of filling in highly filled thermoplastics. Method description and modeling, *Vysokomolekuljarnye Soedineniya*, vol. 28, pp. 321-328.
- Yanagioka, M.; Frank, C.W.** (2008): Effect of Particle Distribution on Morphological and Mechanical Properties of Filled Hydrogel Composites; *Macromolecules*,

vol. 41, no. 14, pp. 5441-5450.

Wu, G.; Lin, Q. J.; Zheng, M. Z. (2006): Correlation between percolation behavior of electricity and viscoelasticity for graphite filled high density polyethylene, *Polymer*, vol. 47, no. 7, pp. 2442–2447.

Zidek, J.; Kucera, J.; Jancar, J. (2010): Model of Random Spatial Packing of Rigid Spheres with Controlled Macroscopic Homogeneity, *CMC: Computer, Materials & Continua*, vol. 16, no. 1, pp. 51-74.